Vol. 46, No. 4 (2024) 570-588, DOI: 10.24874/ti.1670.04.24.07

Tribology in Industry

www.tribology.rs

RESEARCH

Friction and Wear of DLC Coating Deposited on M2 Steel via µW-PECVD Against 100Cr6 Steel with Different Normal Loads and Sliding Speeds Under Dry and Lubrication Conditions

Nay Win Khun[a,*], Anne Neville[b], Ivan Kolev[c], Hongyuan Zhao[b]

[a]*School of Mechanical and Aerospace Engineering, Nanyang Technological University, 50 Nanyang Avenue, Singapore 639798,*
[b]*School of Mechanical Engineering, University of Leeds, Leeds LS2 9JT, UK,*
[c]*IHI Hauzer Techno Coating, Velno 5928 LL, The Netherlands.*

Keywords:

DLC coating
µW-PECVD
Lubrication
Friction
Wear

* Corresponding author:

Nay Win Khun
E-mail: khunnaywin@gmail.com

Received: 28 April 2024
Revised: 20 June 2024
Accepted: 9 July 2024

A B S T R A C T

The friction and wear of diamond-like carbon (DLC) coating deposited on a M2 steel substrate (DLC-Steel) via microwave excited plasma enhanced chemical vapor deposition (µW-PECVD) against a 100Cr6 steel ball without or with an Asian Formulated Oil (AFO) were systematically investigated with different normal loads and sliding speeds. Under a dry condition, the DLC-Steel exhibited an increase in its wear with an increased normal load from 1 to 5 N, while its wear increased with an increased sliding speed from 1 to 3 cm/s and turned to decrease with a further increased sliding speed to 5 cm/s. The increased wear of the DLC-Steel resulted in its increased friction via an increase in contact between two rubbing surfaces during dry sliding. However, the DLC-Steel exhibited a decrease in its friction with an increased normal load or sliding speed under a lubrication condition, although it did not have any measurable wear for all the normal loads and sliding speeds. It could be concluded that the µW-PECVD-DLC coating could effectively prevent its underlying steel substrate from abrasive wear for all the normal loads and sliding speeds under both dry and lubrication conditions.

1. INTRODUCTION

An extensive use of internal combustion (IC) engines in various industries such as transportation, energy and power, oil and gas, agriculture, construction, households, etc. is a major account for a massive emission of CO_2 gas that greatly contributes to global warming and climate change [1-3]. Reducing CO_2 gas emissions in IC engines requires a reduction in fuel consumption, which relies on a reduction in friction losses in engine tribo-components (ETCs) such as cams, followers, piston rings, cylinder bores/liners, crankshafts, camshafts,

etc. [1,4]. Reducing friction and wear of ETCs is beneficial for reducing not only environmental pollution via reduction of CO_2 gas emissions in IC engines but also environmental noise levels by improving the quality, performance, durability, and service life of IC engines [1,5,6]. It is clear that high fuel consumption is a major source of not only climate change, which severely impacts public health, biodiversity, and economic stability, but also non-renewable energy resource depletion, which becomes a global challenge for the ever-growing fuel economy [1,4,7,8]. For these reasons, a major goal of "sustainable green mobility" is importantly set to reduce the environmental impact of "mobility" in terms of energy consumption, emission, pollution, and noise [1,9,10]. Therefore, an effective reduction in the friction and wear of ETCs is the best solution for reducing fuel consumption and CO_2 gas emissions in IC engines and thereby improving global warming, energy conservation, and fuel economy for a more sustainable and greener world. Such a goal can be achieved by developing low friction and high wear resistant materials or coatings for ETCs [1,2,5].

Steels have been commonly used for making ETCs because of their high mechanical strength, high thermal conductivity, and relatively low production costs [11]. In addition, steel's various forms and alloys offer different properties to meet a wide range of ETC applications [11]. However, the relatively high friction and wear of steels are major drawbacks for their durability, performance, and service life, which in turn contribute to a great financial loss in various industries where IC engines are widely used [11,12].

DLC is an amorphous material mainly composed of carbon atoms in sp^2 or sp^3 hybridization [1]. Its rigid sp^3 bonded cross-linking structure is responsible for its high hardness and thereby high abrasive wear resistance, while the formation of its easily sheared graphitic layers during dry sliding makes it low in friction [11,13]. Therefore, a development of low friction and high wear resistant DLC coatings has nowadays become an important strategy to effectively reduce the friction and wear of ETCs modified with them [1,13-15].

ETCs operated in extreme environments such as high temperatures and loads demand thick DLC coatings with strong adhesion for their durability and service life [14,15]. It is, however, well known that DLC coatings have high residual stresses, thereby poor adhesion strength with their underlying substrates, especially with metal substrates, due to a significant difference in coefficients of thermal expansion between DLC and metal, and a very limited thickness of a few hundred "nm" [16,17]. Even the thickness of commercially deployed DLC coatings is not much thicker than a few hundred "nm". Because of these reasons, DLC coatings are very successful for wear testing in laboratories, but often fail in field applications [18]. Therefore, a successful deposition of thick DLC coatings on steel substrates and designing them to survive in extreme environments have become challenges for tribologists and engine makers, which means that research and development of DLC coatings are still necessary to achieve their thickness of above "1 μm".

Generally, physical vapor deposition (PVD) produces thinner DLC coatings than chemical vapor deposition (CVD), if considered from the point of kinetic energies of film-forming species, because a much more energetic bombardment of film-forming species during PVD induces higher residual stresses in the coatings and hence greatly limits the coating thickness [19,20]. It is possible with CVD to produce thicker DLC coatings, but with lower sp^3 contents and densities due to the insufficient energetic bombardment of film-forming species during CVD [19,20]. As a result, advances in manufacturing technologies are always sought to advance DLC coatings with the aim of overcoming their drawbacks. A recent development of μW-PECVD can give rise to better qualities of DLC coatings because microwave discharge induces a higher degree of ionization and hence higher rates of reactions between chemical species in plasma than dc and rf discharges [21-23]. It is therefore expected that μW-PECVD could produce DLC coatings with higher thickness and better tribological performance, and such μW-PECVD-DLC coatings should be further researched to get them advanced in ETC applications by performing their process-structure-performance relationships.

Various lubricants, which can effectively reduce the friction and wear of ETCs, are commercially available for IC engines depending on their specific applications [1,11,12]. Steels used in ETCs highly demand external lubricants for reducing their high friction and wear and extending their service life [1,11,12,24]. Therefore, implementing ETCs with low friction and high wear resistant DLC coatings together with lubricants can be a potential solution for effective improvements in their friction and wear losses, and thereby reducing fuel consumption and CO_2 gas emissions in IC engines for greener mobility.

A fundamental understanding of the friction and wear of μW-PECVD-DLC coatings under dry and lubrication conditions is relatively important to successfully introducing μW-PECVD as a potential manufacturing technology for the fabrication of low friction and high wear resistant DLC coatings. Khun et al. [23] successfully deposited thick DLC coatings on steel substrates via μW-PECVD and investigated their structural and tribological properties with different substrate biases. A few researchers also developed DLC coatings by μW-PECVD to investigate their structural and mechanical properties [21,22,25]. However, available data on the tribological properties of DLC-Steel fabricated by μW-PECVD, especially without or with lubricants, are very limited in the literature, although tribochemical interactions of DLC coatings produced using various manufacturing technologies with various lubricants have been widely studied and reported [1,26]. Therefore, it deserves to investigate their friction and wear behaviour with respect to normal load and sliding speed under dry and lubrication conditions since their tribological performance can greatly vary with different normal loads, sliding speeds, and lubricants, which has not been widely reported in the literature yet. Such investigation will be very useful for tribologists, engine makers, and lubricant developers.

In this study, DLC coating was deposited on a high speed M2 steel substrate via μW-PECVD and its friction and wear against a 100Cr6 steel ball were systematically investigated under dry and lubrication conditions by varying normal loads of 1–5 N and sliding speeds of 1–5 cm/s. Prior to the DLC coating deposition, a tungsten carbide interlayer was introduced between the coating and steel substrate to achieve a high coating thickness by reducing residual stress in the coating and promoting coating adhesion [23]. A 100Cr6 steel ball was used to resemble a tribo-pair of DLC-Steel/Steel. An Al_2O_3 ball was also used in order to discriminate between the wear of bare M2 Steel (B-Steel) generated by 100Cr6 steel and Al_2O_3 balls. The B-Steel was used as a reference material.

2. EXPERIMENTAL DETAILS

2.1 Coating deposition

DLC coating was deposited on a high speed M2 steel substrate via μW-PECVD (Hauzer techno flexi coat® 850 system). Prior to the DLC deposition, the steel substrate fixed on two-fold rotation cylinders (dummies) was cleaned by Ar+ plasma sputtering. Acetylene (C_2H_2+Ar, C_2H_2: 50%) was used as a gas precursor. The detailed μW-PECVD process parameters of the DLC coating are presented in Table 1. Two microwave sources of 2.45 GHz, about 380 mm apart, were located in the center of the 900 mm tall back wall of the chamber. The distance between the sample surface and the microwave source was about 160 mm. A tungsten carbide interlayer with 0.5–0.7 μm in thickness was introduced between the DLC coating and steel substrate using a sputtering system. The steel substrates were mechanically polished by hand using 400, 800, 1000, and 1200 grit papers before the DLC deposition. The DLC coating had a uniform thickness of about 1.5±0.3 μm [23].

Table 1. μW-PECVD process parameters of DLC coating.

μW-PECVD process parameters	
Microwave power	1000 W
C_2H_2 ratio	45%
Gas flow rate	640 sccm
Gas pressure	1.2 Pa
Deposition time	15 min
DC substrate bias	-200V
Substrate rotation	1 rpm

2.2 Characterization

B-Steel and DLC-Steel were analyzed using various characterization techniques, as presented below.

Their surface morphologies and topographies were studied via scanning electron microscopy (SEM, JEOL-JSM-5600LV), surface profilometry (Talyscan 150) with a diamond stylus of 4 μm in diameter, and optical microscopy (OM, Zeiss Axioskop 2, JVC color video camera). For the SEM observation, they were coated with a thin gold layer to avoid a charging effect. Three measurements on each sample were carried out to average an arithmetic average surface roughness (R_a).

Their chemical compositions were measured via energy dispersive X-ray spectroscopy (EDX) attached to SEM.

Their bonding structures were evaluated via micro-Raman spectroscopy (Renishaw RM1000) with a 632 nm line excited by a He-Ne laser in a range of 500–3300 cm^{-1}.

Their tribological properties were investigated using a ball-on-disc micro-tribological test (CSM) by sliding against alumina (Al_2O_3) or 100Cr6 steel balls of 6 mm in diameter without or with AFO in a circular path of 1.5 mm in radius for 70,000 laps (660 m) at different sliding speeds of 1–5 cm/s under different normal loads of 1–5 N. The lubricant used in this experiment was a commercially available AFO that was supplied by Infineum UK Limited. Three measurements per sample were carried out to get average tribological properties. The widths and depths of their wear tracks were measured via surface profilometry and white-light confocal imaging profilometry to calculate their wear volumes.

3. RESULTS AND DISCUSSION

3.1 Morphology, topography, and chemical composition of DLC coating

Figure 1a shows the surface morphology of the DLC coating, on which small grains can be seen. No observation of pinhole defects on its surface is indicative of its high continuity and density [27,28].

Figure 1b shows the EDX spectrum of the DLC coating, measured on its surface, with several peaks of Au, Ar, W, and C elements. The Au peak is attributed to a gold layer coated on the DLC coating for the SEM observation. The Ar peak comes from Ar atoms incorporated in the DLC structure. The W peak probably results from the underlying tungsten carbide interlayer, implying that a certain transparency of the DLC coating allows the X-ray to penetrate the interlayer through it during the EDX measurement [29,30]. The interaction volume of the X-ray should be taken into account in detecting W atoms from the interlayer. In addition, a certain diffusion of W atoms through the interlayer to the DLC coating or a resputtering effect of the interlayer via high energetic bombardment of positive ions at the high negative substrate bias of -200 V during the μW-PECVD is possible, which contributes to the W peak [31,32]. The C peak is attributed to C atoms, mainly from the C matrix.

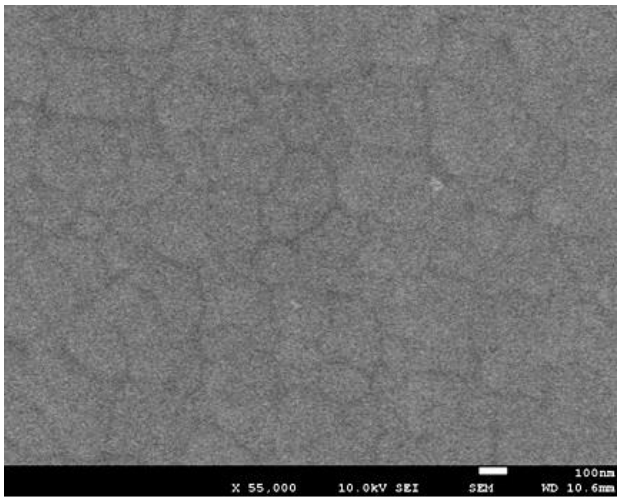

(a)

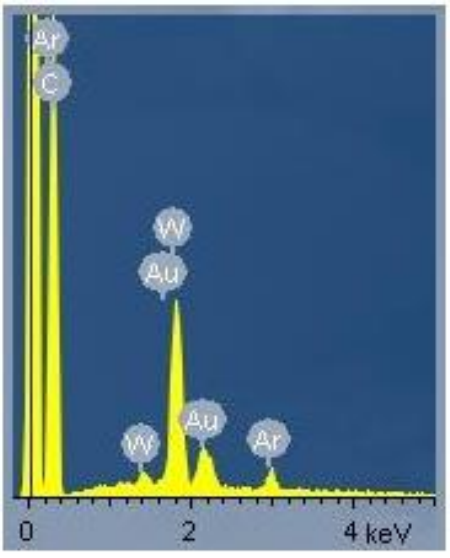

(b)

Fig. 1. (a) Surface morphology of DLC coating and (b) its EDX spectrum.

Mechanical polishing of a steel surface to achieve a mirror-like surface with "nm" surface asperities is indeed costly and time consuming. In this study, polished B-Steel with the lack of a mirror-like surface is used as a substrate to understand the wear protective performance of the DLC coating over such a substrate surface under dry and lubrication conditions.

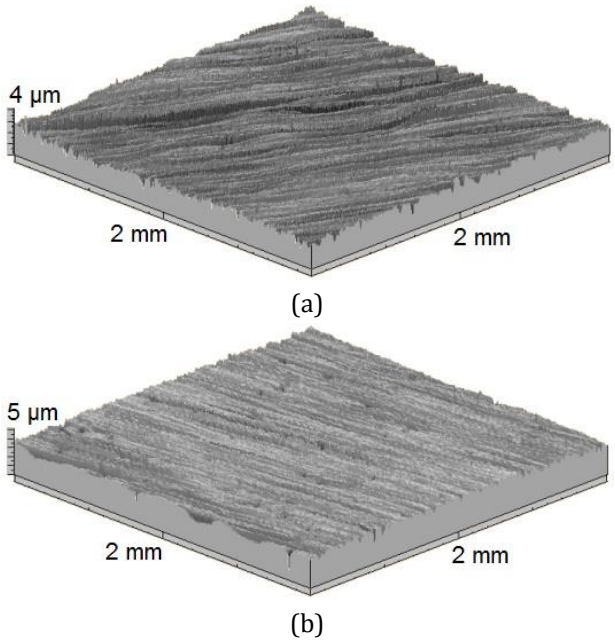

Fig. 2. Surface topographies of (a) polished B-steel and (b) DLC-Steel measured in a scan area of 2 mm × 2 mm.

Figure 2a shows the surface topography of the polished B-Steel, on which abrasive lines with deep channels left by the mechanical polishing are found. When the surface of the same B-Steel is coated with the DLC coating, the DLC-Steel has a relatively smoother surface with shallow channels, as found in Figure 2b, which is confirmed by its smaller R_a value of 0.28±0.08 μm compared to 0.35±0.13 μm of the polished B-Steel. All the tribo-tests were carried out on these surfaces.

3.2 Friction and wear of B-Steel and DLC-Steel under dry and lubrication conditions

Figure 3a presents the friction coefficients of the B-Steel and DLC-Steel tested against a 100Cr6 steel ball without or with AFO at a sliding speed of 3 cm/s under a normal load of 3 N. The friction and wear data of the B-Steel under dry and lubrication conditions are used as a reference. The friction coefficient of the B-Steel tested dry against a 100Cr6 steel ball at 3 cm/s under 3 N is 0.526 (Figure 3a), while its friction coefficient against an Al_2O_3 ball under the same conditions is 0.748±0.025, which is 42.2% higher than its friction coefficient against a 100Cr6 steel ball. Its wear volumes tested dry against 100Cr6 steel and Al_2O_3 balls at 3 cm/s under 3 N are $6.06±1.23×10^{-12}$ m^3 and $83.34±13.79×10^{-12}$ m^3, respectively, indicating that the repeated dry sliding of the much harder Al_2O_3 ball generates its much higher abrasive wear [33]. Generally, a larger contact between two rubbing surfaces generates higher friction via a larger number of contact junction points between them to adhere to each other [34,35]. Under 3 N, the wrapping contact of the B-Steel on an Al_2O_3 ball via its preferential surface deformation contributes to its higher friction compared to its possible flat contact with a 100Cr6 steel ball via their surface deformation, while its wrapping contact on an Al_2O_3 ball via its higher surface wear gives rise to its higher friction than its flat contact with a 100Cr6 steel ball via their surface wear.

In Figure 3a, the friction coefficient of the DLC-Steel tested dry against a 100Cr6 steel ball at 3 cm/s under 3 N is 0.222, which is 57.8% and 70.3% lower than those of the B-Steel against 100Cr6 steel and Al_2O_3 balls under the same conditions, respectively. The wear volume of the DLC-Steel tested dry against a 100Cr6 steel ball is $0.90±0.14×10^{-12}$ m^3, which is 85.1% and 98.9% lower than those of the B-Steel against 100Cr6 steel and Al_2O_3 balls, respectively, implying that the higher wear resistant DLC coating effectively prevents its underlying steel substrate from abrasive wear during prolonged dry sliding. The apparently lower friction of the DLC-Steel against a 100Cr6 steel ball than that of the B-Steel against the same steel ball (Figure 3a) under a dry condition is mainly due to its low friction DLC coating [36]. In addition, the existence of the much harder DLC coating between the softer steel substrate and ball eliminates a direct metal-on-metal contact during the dry sliding, resulting in lower friction for the DLC-Steel. Besides, the lower friction and higher wear resistance of the DLC coating than those of the M2 and 100Cr6 steels result in a smaller contact between two rubbing surfaces by effectively preventing their abrasive wear and thereby the lower friction of the DLC-Steel [37]. Furthermore, mechanical interlocking between mating surface asperities induces high

friction, so the lower friction of the DLC-Steel can also be related to its smoother surface compared to the rougher surface of the B-Steel [34,38]. Therefore, it can be deduced that the existence of the DLC coating with lower friction, higher wear resistance, and lower surface roughness on the DLC-Steel apparently lowers its friction than that of the B-Steel during the dry sliding against a 100Cr6 steel ball, as found in Figure 3a.

The B-Steel tested against 100Cr6 steel (Figure 3a) and Al_2O_3 balls with AFO at 3 cm/s under 3 N has 81.6 and 82.1 % lower friction coefficients of 0.097 and 0.133±0.018, respectively, compared to its friction coefficients without AFO, indicating that the use of the AFO results in an over 80% decrease in its friction during the rubbing contact with both 100Cr6 steel and Al_2O_3 balls. It can be imagined that deep channels on the B-Steel surface (Figure 2a) serve as reservoirs to continuously supply AFO and effectively lubricate rubbing surfaces during sliding, in addition to the effective lubricating effect of the AFO [39]. Under the lubrication condition, the friction of the B-Steel against a 100Cr6 steel ball is 31.6% lower than its friction against an Al_2O_3 ball. It indicates that the use of the 100Cr6 steel ball with AFO gives rise to the lower friction of the B-Steel by generating the lower wear of both rubbing surfaces. The wear volume of the B-Steel tested against an Al_2O_3 ball with AFO is $0.70\pm0.17\times10^{-12}$ m^3, which is 88.4% and 99.2% lower than its wear volumes against 100Cr6 steel and Al_2O_3 balls without AFO, respectively, although its wear against a 100Cr6 steel ball with AFO is not measurable as a result of the effective lubricating effect of the AFO. It is, however, found that the much harder Al_2O_3 ball can still generate the higher abrasive wear of the B-Steel than the softer 100Cr6 steel ball even under the lubrication condition [33].

The friction coefficient of the DLC-Steel tested against a 100Cr6 steel ball with AFO at 3 cm/s under 3 N is 0.089 (Figure 3a), which is 59.9% lower than its friction coefficient without AFO and 8.2% lower than that of the B-Steel against a 100Cr6 steel ball with AFO. The DLC-Steel tested against a 100Cr6 steel ball has apparently lower friction under the lubrication condition than under the dry condition, as well as lower friction than that of the B-Steel against the same steel ball even under the lubrication condition because the smoother surface of its DLC coating improves a lubricating layer and its bearing surface for more effective lubrication with AFO [40,41]. Nevertheless, the wear of both B-Steel and DLC-Steel against a 100Cr6 steel ball with AFO is not measurable.

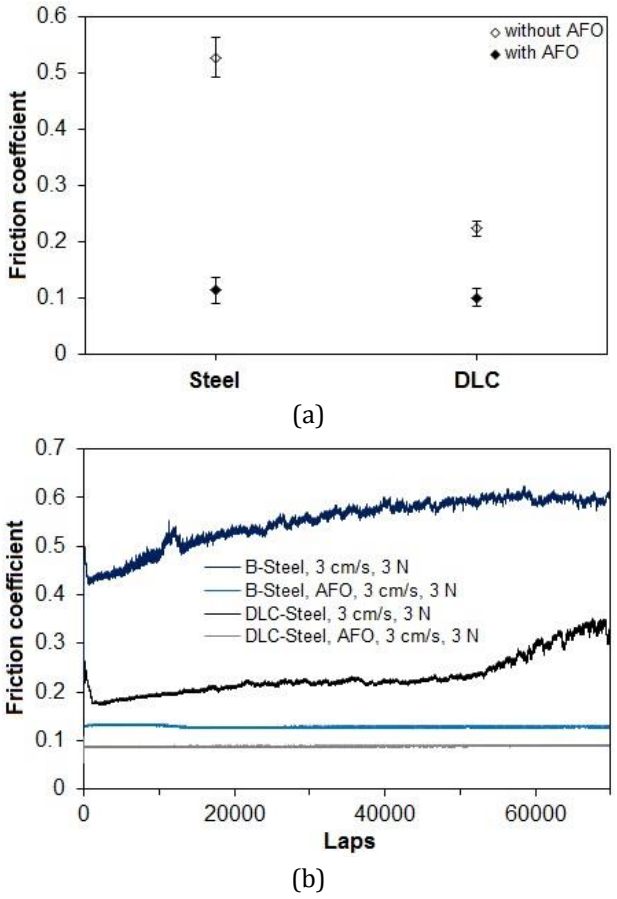

Fig. 3. (a) Friction coefficients of B-steel and DLC-Steel tested against a 100Cr6 steel ball without or with AFO at a sliding speed of 3 cm/s under a normal load of 3 N. (b) Their friction coefficients as a function of the number of laps.

Figure 3b illustrates the friction coefficients of the B-Steel and DLC-Steel tested against a 100Cr6 steel ball without or with AFO at 3 cm/s under 3 N as a function of the number of laps. Under a dry condition, the B-Steel exhibits an apparent increase in its friction with increased laps as a result of its increased surface wear. However, the DLC-Steel has a slight increase in its friction with increased laps up to about 52,000 laps and then an apparent increase in its friction for the rest after a breakdown of its DLC coating. Under a lubrication condition (Figure 3b), both B-Steel and DLC-Steel exhibit much lower and much more stable friction throughout the wear tests, but the DLC-Steel has a lower

trend of friction coefficient versus laps. It confirms that the AFO is an effective lubricant for both B-Steel and DLC-Steel and is more effective with the DLC-Steel, especially against the 100Cr6 steel ball.

Figure 4a shows the wear morphology and topography of the B-Steel tested dry against a 100Cr6 steel ball at 3 cm/s under 3 N. Although the repeated dry sliding of the 100Cr6 steel ball on the B-Steel generates the wear of both, the lower wear resistance of the 100Cr6 steel ball than that of the B-Steel results in its preferential abrasive wear, so that the wear track of the latter is not very significant in Figure 4a. As a result, the wear of both B-Steel and 100Cr6 steel balls generates a significant amount of wear debris that is densely compacted on the wear track of the higher wear resistant B-Steel to form tribolayers during the dry sliding, as found in Figure 4a [34,42].

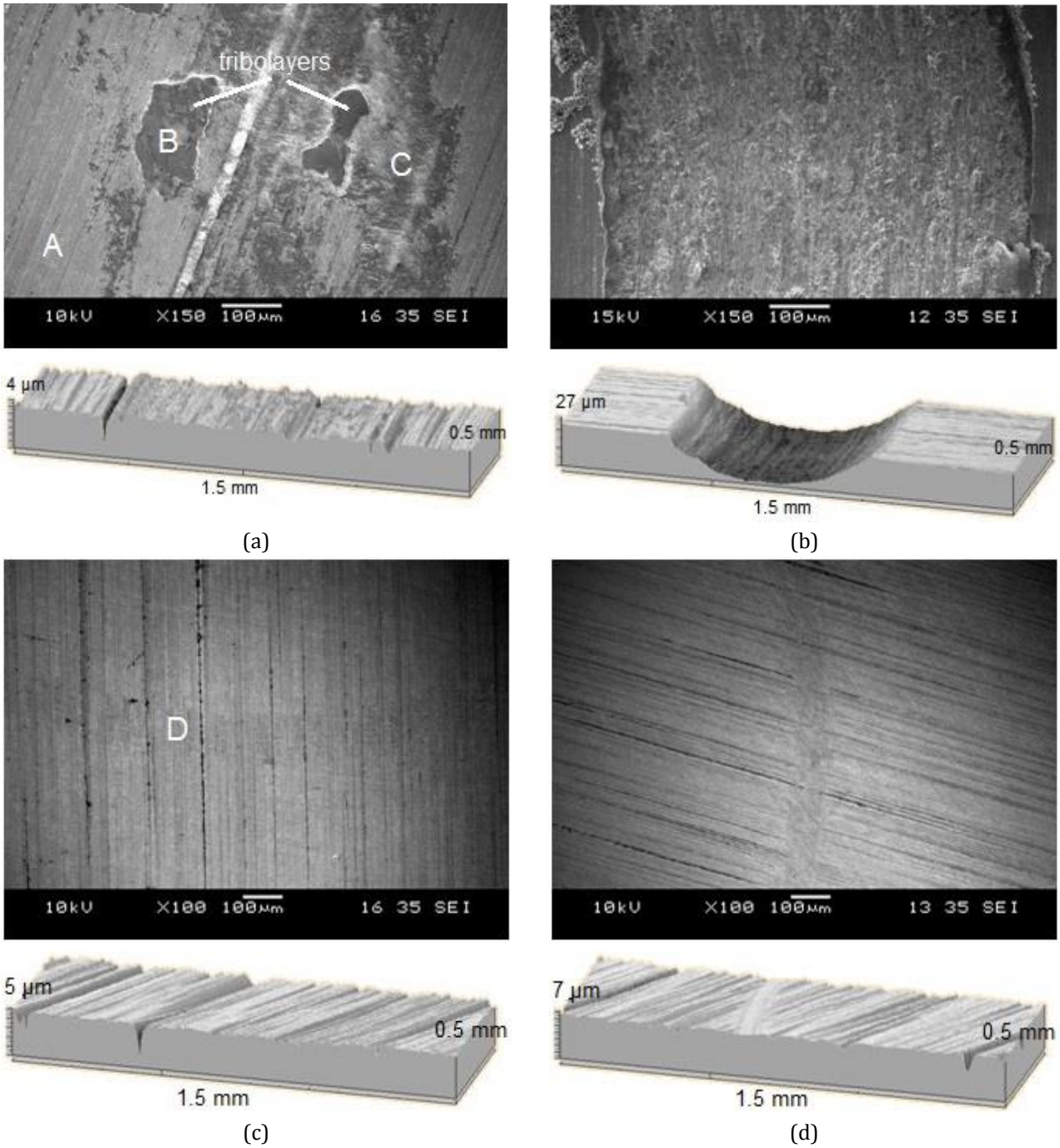

Fig. 4. Wear morphologies (above) and topographies (below) of B-steel tested against (a and c) 100Cr6 steel and (b and d) Al_2O_3 balls (a and b) without or (c and d) with AFO at a sliding speed of 3 cm/s under a normal load of 3 N.

Figure 4b shows the wear morphology and topography of the B-Steel tested dry against an Al_2O_3 ball at 3 cm/s under 3 N, from which its much more significant wear with a much larger wear track is found. It confirms that the much harder Al_2O_3 ball generates much higher abrasive wear of the B-Steel during dry sliding than the 100Cr6 steel ball, as the repeated dry sliding of the 100Cr6 steel ball on the higher wear resistant B-Steel results in its preferential abrasive wear [33]. In Figure 4b, the repeated dry sliding of the Al_2O_3 ball does not generate any surface material spallation or micro-cracks associated with fatigue wear on the wear track of the B-Steel except abrasive wear [43]. As shown by the comparison of Figures 4a and 4b, the much higher abrasive wear of the B-Steel against an Al_2O_3 ball does not allow the formation of thick tribolayers on its wear track via its faster surface material removal. Instead, smaller tribolayers are formed on its wear track (Figure 4b) compared to those on its wear track against a 100Cr6 steel ball (Figure 4a).

Figure 4c shows the wear morphology and topography of the B-Steel tested against a 100Cr6 steel ball with AFO at 3 cm/s under 3 N, on which an unmeasurable wear track is found. However, the B-Steel tested against an Al_2O_3 ball under the same conditions has a more apparent and measurable wear track, as found in Figure 4d, confirming that the repeated sliding of the much harder Al_2O_3 ball can still generate its wear even under the lubrication condition. Nevertheless, the wear of the B-Steel tested against 100Cr6 steel and Al_2O_3 balls with AFO (Figures 4c and 4d) is much lower than its wear against the same balls without AFO (Figures 4a and 4b), confirming that the abrasive wear of the B-Steel is effectively prevented by the AFO during prolonged sliding, although its abrasive wear is influenced by the type of its counter balls used.

Figure 5a and its inset show the wear morphology and topography of the DLC-Steel tested dry against a 100Cr6 steel ball at 3 cm/s under 3 N, respectively, on which a wear track with an abrasive wear scar can be seen, but a significant removal of surface materials is not found. The comparison of Figures 4a and 5a confirms that the DLC-Steel has apparently lower wear than the B-Steel under a dry condition as a result of the effective wear protective performance of its DLC coating. In Figure 5b, the DLC-Steel against a 100Cr6 steel ball with AFO at 3 cm/s under 3 N has unmeasurable wear, which confirms that the AFO is very effective to prevent the abrasive wear of the DLC-Steel during prolonged sliding.

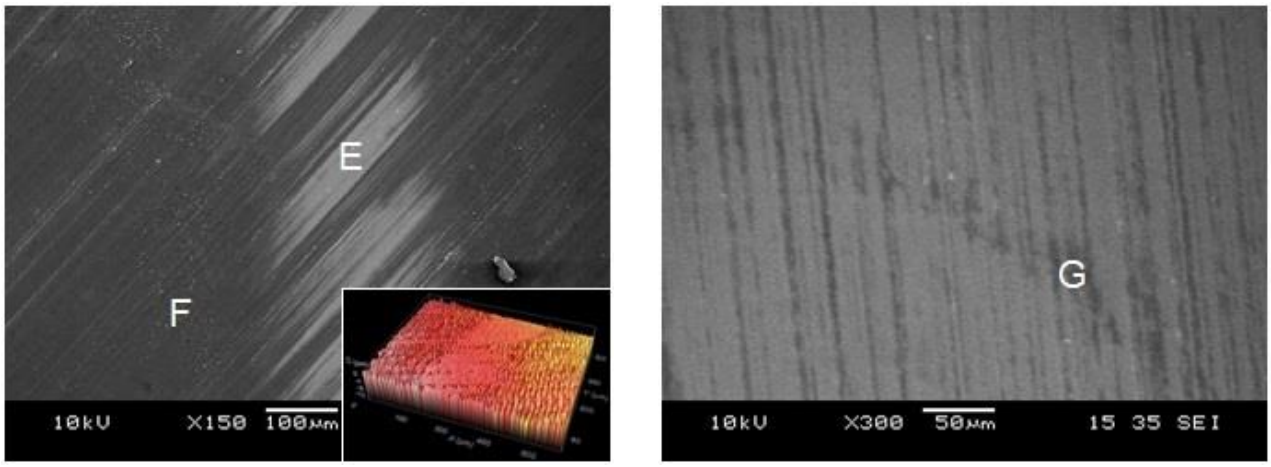

(a) (b)

Fig. 5. Wear morphologies of DLC-steel tested against a 100Cr6 steel ball (a) without or (b) with AFO at a sliding speed of 3 cm/s under a normal load of 3 N. The inset shows its respective wear topography.

Figure 6a shows the wear morphology of the 100Cr6 steel ball rubbed on the B-Steel without AFO at 3 cm/s under 3 N. The severe abrasive wear of the 100Cr6 steel ball with ploughed furrows confirms that its repeated dry sliding on the rougher surface of the higher wear resistant B-Steel results in its preferential abrasive wear [34,44]. It also confirms that the preferential wear of the 100Cr6 steel ball is mainly responsible for the formation of thick

tribolayers on the wear track of the B-Steel under a dry condition (Figure 4a). Under the same conditions, the repeated dry sliding of the much higher wear resistant Al_2O_3 ball on the B-Steel results in the preferential wear of the latter, which is confirmed by its much smaller wear scar (Figure 6b) compared to that of the 100Cr6 steel ball (Figure 6a). Abrasive lines on the wear scar of the Al_2O_3 ball (Figure 6b) are indicative of its suffering from dry abrasive wear [11,44]. The brown colored materials adhered to the wear scar of the Al_2O_3 ball are probably oxidized materials transferred via the wear of the B-Steel [45].

As shown in Figures 6a and 6c, the low friction and high wear resistant DLC coating effectively lowers the wear of its steel substrate and counter steel ball but still results in the preferential abrasive wear of its counter steel ball during dry sliding. Normally, a rough surface of a solid material can serve as an abrading surface to cause high abrasive wear of its counter material during rubbing each other [34,46]. Therefore, the DLC-Steel with a smoother surface gives rise to lower abrasive wear of the counter 100Cr6 steel ball than the B-Steel with a rougher surface. However, abrasive lines are still observed on the wear scar of the 100Cr6 steel ball (Figure 6c), which imply that the 100Cr6 steel ball rubbed on the DLC-Steel under a dry condition still suffers abrasive wear attributed to the rough surface of the latter [34,44].

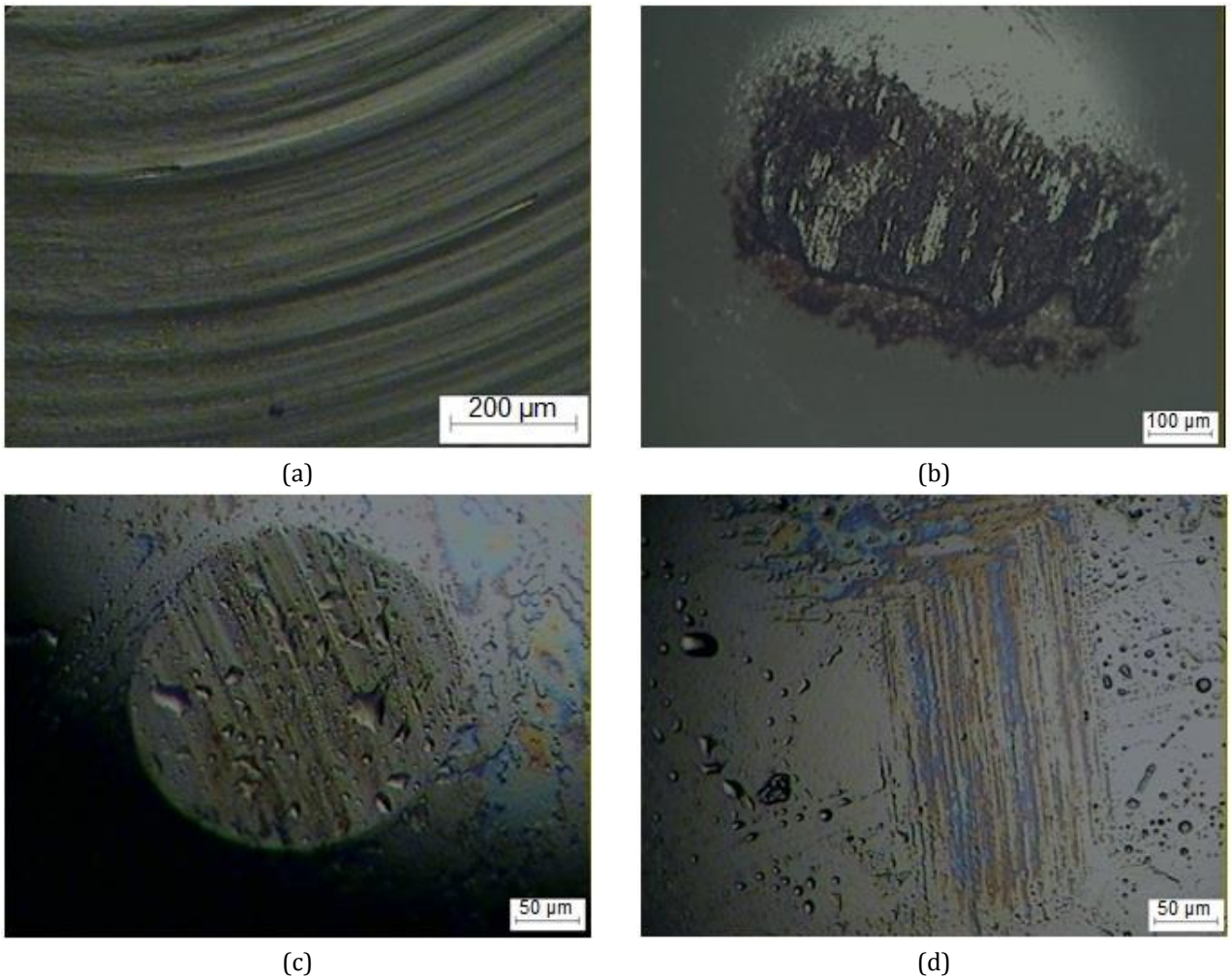

Fig. 6. Wear morphologies of (a) 100Cr6 steel ball rubbed on B-Steel without AFO, (b) Al_2O_3 ball rubbed on B-Steel without AFO, (c) 100Cr6 steel ball rubbed on DLC-Steel without AFO, and (d) 100Cr6 steel ball rubbed on B-Steel with AFO at a sliding speed of 3 cm/s under a normal load of 3 N.

Figure 6d shows the wear morphology of the 100Cr6 steel ball rotated on the B-Steel with AFO at 3 cm/s under 3 N, on which no apparent wear scar is found, but a tribofilm formed by the AFO can be seen [26]. It was found that the Al_2O_3 ball rubbed on the B-Steel with AFO under the same

conditions had a similar tribofilm and no apparent wear scar. The wear scar of the 100Cr6 steel ball rubbed on the DLC-Steel with AFO cannot be clearly identified. The results clearly confirm that the AFO effectively prevents the abrasive wear of not only both B-Steel and DLC-Steel but also their counter balls during prolonged sliding.

In Figure 7, the DLC-Steel shows a typical Raman spectrum of its DLC coating measured at location "E" in its untested area (Figure 5a). The Raman spectrum was fitted with two Gaussian peaks for G (graphite) and D (disordered) peaks [47]. A well-defined appearance of the D peak in the Raman spectrum is indicative of a high amount of aromatic rings in the DLC structure [47]. The G and D peaks exist at 1502.1 cm^{-1} and 1303.9 cm^{-1}, respectively, as their intensity ratio (I_D/I_G) is 0.54.

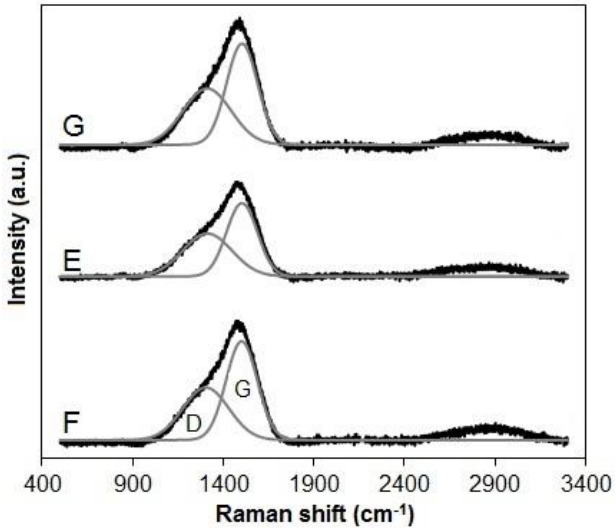

Fig. 7. Raman spectra of DLC-Steel, tested against a 100Cr6 steel ball (E) without or (G) with AFO, measured on locations "F" in untested area and "E" on wear track of Figure 5a, and (c) "G" on wear track of Figure 5b.

The Raman spectrum of the DLC-Steel obtained from location "F" on its wear track without AFO (Figure 5a) is similar to that of its untested area, implying that the DLC coating still remains on its surface even after the prolonged dry sliding for 70,000 laps. Its G and D peak positions slightly shift to higher values of 1502.9 cm^{-1} and 1312.1 cm^{-1}, respectively, while its I_D/I_G slightly increases to 0.59. It suggests that the prolonged dry sliding of the 100Cr6 steel ball on the DLC coating promotes graphitization of the latter via the generation of frictional heat, which contributes to the low friction of the DLC-Steel during the dry sliding [47,48].

In Figure 7, the G and D peak positions of the Raman spectrum measured at location "G" on the wear track of the DLC-Steel with AFO (Figure 5b) are 1502.7 and 1311.1 cm^{-1}, respectively, as its I_D/I_G is 0.56. These Raman parameters are slightly larger than those measured on its untested area and smaller than those measured on its wear track without AFO. It means that the existence of the AFO on the DLC coating during sliding lessens graphitization of the latter by preventing direct contact between two rubbing surfaces and serving as a coolant [47,49]. The Raman results show that the prolonged sliding of the 100Cr6 steel ball more or less induces the surface structural changes of the DLC coating under both dry and lubrication conditions.

Figure 8a shows the EDX spectrum of the B-Steel measured at location "A" in its untested area (Figure 4a), which has several peaks of background chemical elements such as Fe, Cr, W, Mo, C, and V. However, the lack of V, W, and Mo peaks on the EDX spectrum measured at location "B" on the tribolayer (Figures 4a and 8b) and the existence of weaker W and Mo peaks with the lack of V peak on the EDX spectrum measured at location "C" (Figures 4a and 8c) on its wear track without AFO imply that the tribolayers are mainly composed of wear debris produced by the preferential wear of the 100Cr6 steel ball during dry sliding. An additional O peak is found on its wear track without AFO, which can be related to an oxidation process that occurred during dry sliding [34].

The EDX spectrum of the B-Steel measured at location "D" on its wear track with AFO (Figures 4c and 8d) has the same background chemical elements found in its untested area (Figure 8a), which implies that the AFO effectively prevents the abrasive wear of both rubbing surfaces. An additional Ca peak detected on its wear track with the AFO probably comes from Ca-containing detergent additives in the AFO.

Figure 9a shows the EDX spectrum of the DLC-Steel measured at location "F" in its untested area (Figure 5a) with C, Ar, W, and Au elements. The C peak mainly comes from the DLC coating, as the Ar peak is indicative of the incorporation of Ar atoms in the DLC structure. The W peak results from the tungsten carbide interlayer and diffused W atoms in the DLC coating while the Au peak is attributed to a gold layer on the DLC coating.

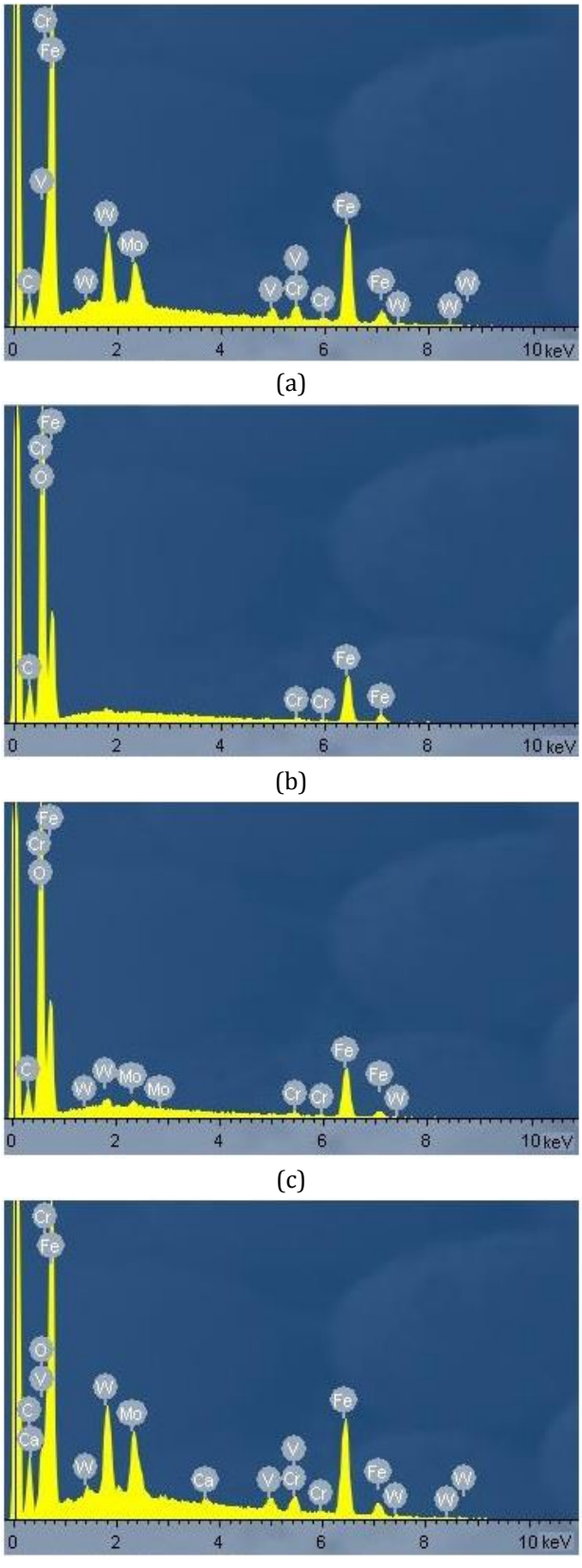

Fig. 8. EDX spectra of B-Steel, tested (b, and c) without or (d) with AFO, measured on locations (a) "A" in untested area, (b) "B" on tribolayer, and (c) "C" on wear track of Figure 4a and (d) "D" on wear track of Figure 4c.

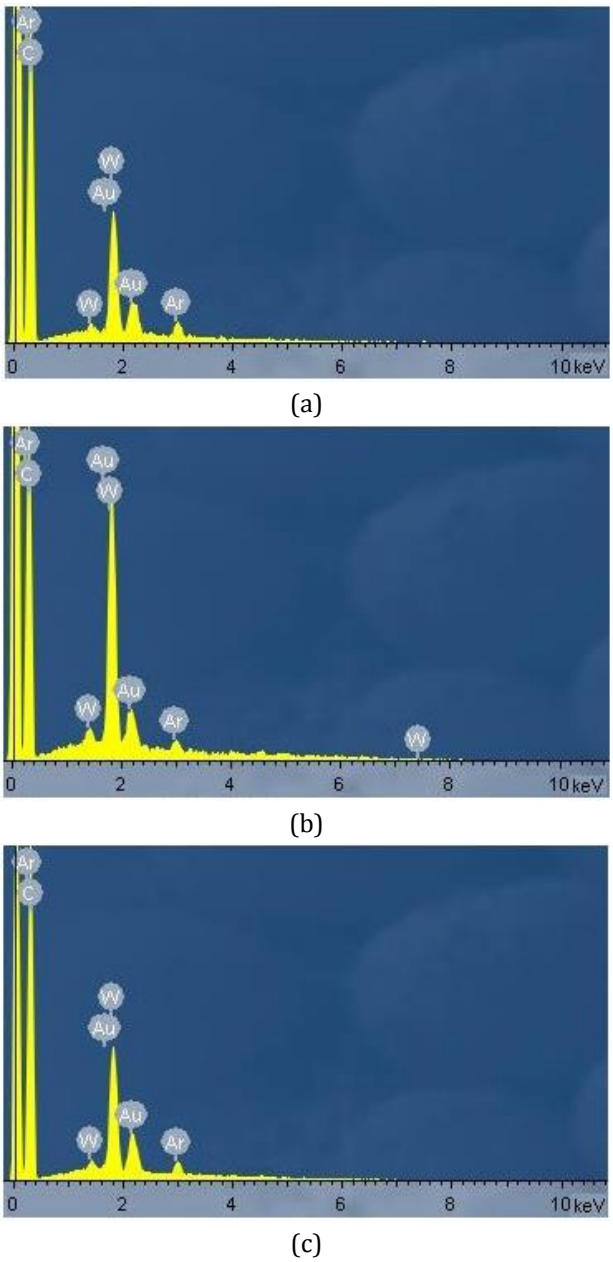

Fig. 9. EDX spectra of DLC-Steel, tested (b) without or (c) with AFO, measured on locations (a) "F" in untested area and (b) "E" on wear track of Figure 5a, and (c) "G" on wear track of Figure 5b.

The chemical elements presented in Figure 9a are consistent with those found in Figure 1b. Although the EDX spectrum of the DLC-Steel measured at location "E" on its wear track without AFO (Figures 5a and 9b) has the same chemical elements found in its untested area (Figure 9a), the stronger W peak on its wear track points out that the prolonged dry sliding of the 100Cr6 steel ball more or less wears out its DLC coating, which allows the detection of more W elements from the tungsten carbide interlayer and steel substrate. In addition, Fe and Cr

elements coming from the wear debris of the 100Cr6 steel ball are not apparently detected on its EDX spectrum (Figure 9b). However, no apparent difference in the EDX spectra of the DLC-Steel measured in its untested area (Figure 9a) and wear track with AFO (Figure 9c) clearly implies that the AFO effectively prevents the wear of not only the DLC-Steel but also its counter 100Cr6 steel ball, which is further confirmed by no observation of additional Fe and Cr peaks on the EDX spectrum in Figure 9c. Moreover, the Ca element, which is found on the wear track of the B-Steel with AFO (Figure 8d), is not detected on the wear track of the DLC-Steel with the same AFO (Figure 9c).

3.3 Effect of normal load on friction and wear of DLC-Steel under dry and lubrication conditions

Figure 10a presents the friction coefficients of the DLC-Steel tested against a 100Cr6 steel ball without or with AFO at 3 cm/s under different normal loads of 1–5 N. The friction coefficient of the DLC-Steel tested dry increases from 0.203 to 0.241 (18.7% higher) with an increased normal load from 1 to 5 N, while its wear volume apparently increases from $0.28\pm0.15\times10^{-12}$ m^3 to $1.45\pm0.37\times10^{-12}$ m^3 (417.9% higher). It indicates that the increased wear of the DLC-Steel with an increased normal load increases its friction via increased contact between two rubbing surfaces under a dry condition. It is clear that the use of a higher normal load during dry sliding gives rise to the higher friction and wear of the DLC-Steel in this study [50].

In Figure 10a, the friction coefficient of the DLC-Steel tested with AFO decreases from 0.110 to 0.062 (43.6% lower) with an increased normal load from 1 to 5 N because the use of a higher normal load during the sliding causes more flattening of surface asperities at contact points, which in turn lessens mechanical interlocking between them, improves a lubricating layer and its bearing surface, and thereby promotes effective lubrication with the AFO [51,52].

Figure 10b presents the trends of friction coefficient versus laps of the DLC-Steel tested against a 100Cr6 steel ball without or with AFO at 3 cm/s under different normal loads. Without AFO, the friction of the DLC-Steel under 1 N slightly increases with increased laps due to the steadily increased wear of two rubbing surfaces associated with the prolonged dry sliding. However, the DLC-Steel exhibits a significant increase in its friction under the higher normal loads of 3 N and 5 N after about 52,000 and 50,000 laps, respectively, as a result of the breakdown of its DLC coating, while the coating breakdown happens earlier with the higher normal load. Such a breakdown of the DLC-Steel is not found for the normal load of 1 N, which means that the DLC coating has better wear protective performance during prolonged dry sliding under the lower normal loads. Under a lubrication condition, the DLC-Steel consistently exhibits much more stable and much lower friction during the entire sliding under all the normal loads of 1–5 N, as it has a significant decrease in its friction for all the laps with an increased normal load via promoted lubrication with the AFO associated with its improved bearing surface.

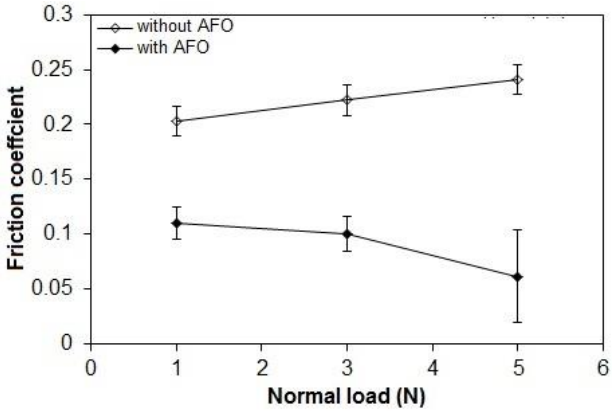

(a)

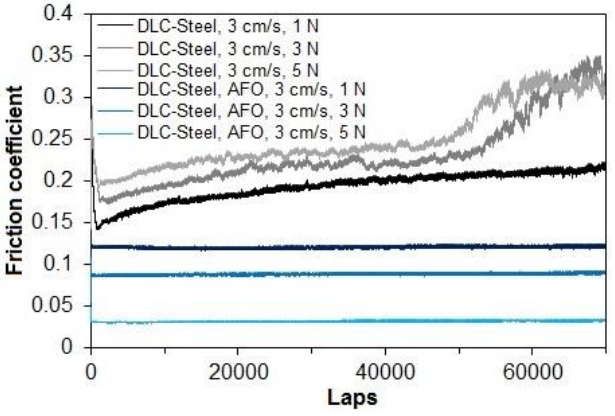

(b)

Fig. 10. (a) Friction coefficients of DLC-Steel tested against a 100Cr6 steel ball without or with AFO at a sliding speed of 3 cm/s under different normal loads of 1–5 N. (b) Its friction coefficients as a function of the number of laps.

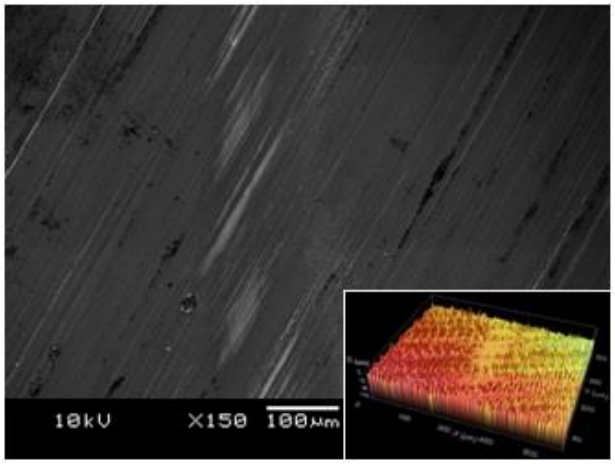

(a)

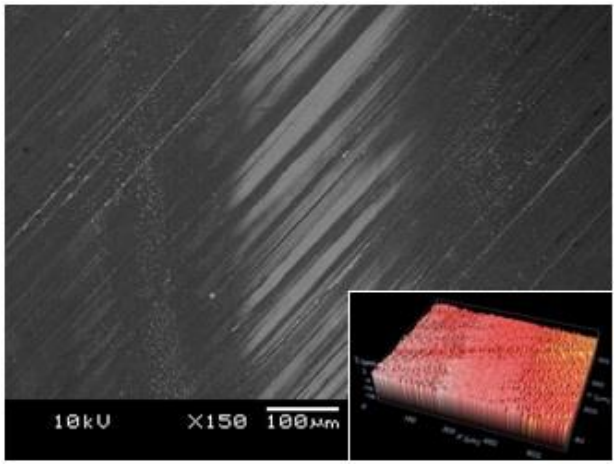

(b)

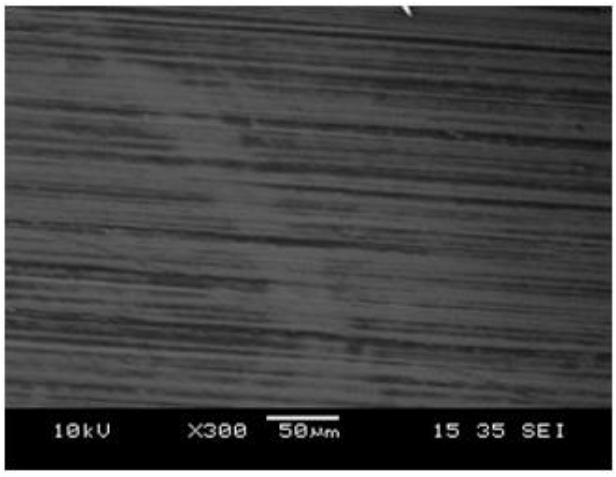

(c)

Fig. 11. Wear morphologies of DLC-Steel tested against a 100Cr6 steel ball (a and b) without or (c) with AFO at a sliding speed of 3 cm/s under normal loads of (a) 1 N and (b and c) 5 N.

Figures 11a and 11b show the wear morphologies of the DLC-Steel tested dry against a 100Cr6 steel ball at 3 cm/s under 1 N and 5 N, respectively. Based on the comparison of Figures 11a, 5a, and 11b, the DLC-Steel has a larger abrasive wear track for a higher normal load but does not have any significant removal of surface materials except for its abrasive wear scar, which confirms that it has higher abrasive wear with a higher normal load under a dry condition.

Figures 5b and 11c show the wear morphologies of the DLC-Steel against a 100Cr6 steel ball with AFO at 3 cm/s under 3 N and 5 N, respectively, on which unmeasurable wear is found for both normal loads. The DLC-Steel has less apparent wear under the higher normal load of 5 N, confirming its better bearing surface for more effective lubrication with the AFO.

3.4 Effect of sliding speed on friction and wear of DLC-Steel under dry and lubrication conditions

Figure 12a shows the friction coefficients of the DLC-Steel tested against a 100Cr6 steel ball without or with AFO at different sliding speeds of 1–5 cm/s under 3 N. The friction coefficients of the DLC-Steel tested dry at 1 cm/s, 3 cm/s, and 5 cm/s under 3 N are 0.213, 0.222, and 0.214, respectively. The DLC-Steel has a 4.2% increase in its friction with an increased sliding speed from 1 to 3 cm/s, and then a 3.6% decrease in its friction with a further increased sliding speed to 5 cm/s. The wear volume of the DLC-Steel increases from $0.53\pm0.10\times10^{-12}$ m^3 to $0.9\pm0.14\times10^{-12}$ m^3 (69.8% higher) with an increased sliding speed from 1 to 3 cm/s and turns to decrease to $0.78\pm0.05\times10^{-12}$ m^3 (13.3% lower) when the sliding speed is further increased to 5 cm/s. It is supposed that the increased vibration of the tribo-system with an increased sliding speed to 3 cm/s probably increases the wear of the DLC-Steel under a dry condition, as the pronounced vibration of the tribo-system with a further increased sliding speed to 5 cm/s decreases its abrasive wear by lessening contact between two rubbing surfaces [53]. Therefore, the increased wear of the DLC-Steel with an increased sliding speed to 3 cm/s increases contact between two rubbing surfaces and, subsequently, its friction, as its decreased wear associated with a further increased sliding speed to 5 cm/s decreases its friction [34,35].

In Figure 12a, the DLC-Steel tested against a 100Cr6 steel ball with AFO under 3 N exhibits a decrease in its friction coefficient from 0.125 to 0.093 (25.6% lower) with an increased sliding

speed from 1 to 5 cm/s. It is therefore supposed that the promoted lubricating layer with a higher sliding speed probably results in more effective separation and lubrication between two rubbing surfaces with the AFO [54,55]. Nevertheless, the DLC-Steel has lower friction for all sliding speeds under a lubrication condition.

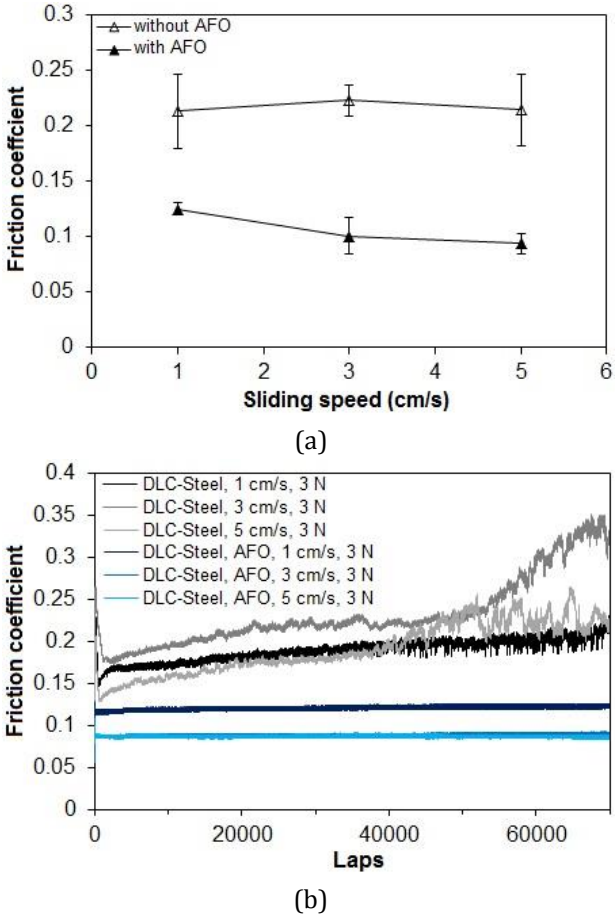

Fig. 12. (a) Friction coefficients of DLC-Steel tested against a 100Cr6 steel ball without or with AFO at different sliding speeds of 1–5 cm/s under a normal load of 3 N. (b) Its friction coefficients as a function of the number of laps.

Figure 12b illustrates the friction of the DLC-Steel tested against a 100Cr6 steel ball without or with AFO at different sliding speeds under 3 N as a function of the number of laps. The DLC-Steel exhibits its most stable friction during the entire dry sliding at the lowest sliding speed of 1 cm/s, probably due to the lowest vibration of the tribo-system and the lowest wear damage to rubbing surfaces. Increasing the sliding speed to 3 cm/s accelerates the abrasive wear of the DLC coating and thereby results in its breakdown at about 52,000 laps, as shown by a significant increase in the friction of the DLC-Steel associated with an increase in the wear of rubbing surfaces. The DLC-Steel tested at 5 cm/s exhibits lower friction for the initial 40,000 laps compared to its friction at 3 cm/s, probably due to the promoted graphitization of the DLC coating associated with higher frictional heat generated during the faster dry sliding [56]. Such frictional heat induced graphitization eventually leads to an earlier breakdown of the DLC coating by degrading its sp^3 bonded cross-linking structure, resulting in the generation of wear debris and a reduction and fluctuation in the friction of the DLC-Steel via its unstable wear after the 40,000 laps (Figure 12b), since wear debris can serve as spacers to prevent a direct solid-solid contact between two rubbing surfaces and slide or roll under a lateral force [34,56,57]. It should also be noted that the more surface strain hardening of its counter 100Cr6 steel ball associated with higher sliding speed is responsible for its lower initial friction through a smaller contact between two rubbing surfaces [58]. The pronounced vibration of the tribosystem can also contribute to its lower initial friction by lessening the interfacial shear strength between two rubbing surfaces [54,55].

In Figure 12b, the DLC-Steel has much lower and much more stable trends of friction coefficient versus laps for all the sliding speeds under the lubrication condition than under the dry condition, as well as a lower trend for the higher sliding speed. It is clear that the sliding speed apparently affects the friction of the DLC-Steel under both dry and lubrication conditions in this study.

Figures 13a and 13b show the wear morphologies of the DLC-Steel tested dry against a 100Cr6 steel ball at 1 cm/s and 5 cm/s under 3 N. The comparison of Figures 13a, 5a, and 13b consistently shows that the abrasive wear of the DLC-Steel increases with an increased sliding speed from 1 to 3 cm/s and then turns to decrease with a further increased sliding speed to 5 cm/s. In Figure 13b, an interacting width of the DLC-Steel with its counter 100Cr6 steel ball at 5 cm/s is relatively wider with a smaller abrasive wear scar compared to its abrasive wear track at 3 cm/s, confirming that the pronounced vibration of the tribo-system associated with 5 cm/s results in the wider interacting width between the DLC-steel and 100Cr6 steel ball with less abrasive wear.

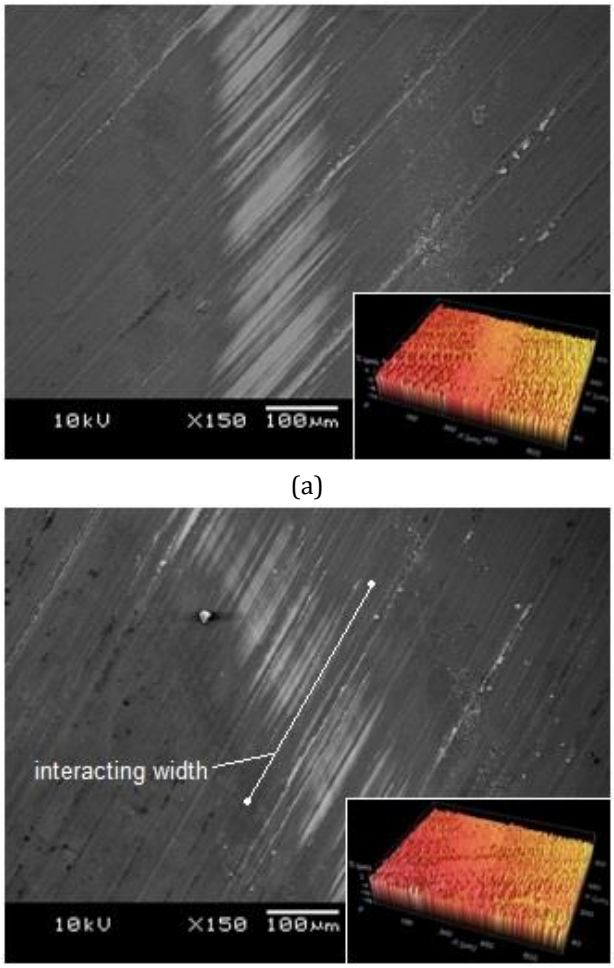

Fig. 13. Wear morphologies of DLC-Steel tested against a 100Cr6 steel ball without AFO at sliding speeds of (a) 1 cm/s and (b) 5 cm/s under a normal load of 3 N.

Based on the presented results, the wear volumes of the DLC-Steel tested dry against a 100Cr6 steel ball at different sliding speeds under different normal loads are not very different from that of the B-Steel generated by an Al_2O_3 ball with AFO, implying that the DLC coating effectively prevents its underlying steel from abrasive wear even under the dry condition. It is therefore not surprising that the DLC-Steel tested against a 100Cr6 steel ball with AFO does not have any measurable wear for all the normal loads and sliding speeds.

A decrease in the friction of the DLC-Steel is slower with an increased normal load from 1 to 3 N and faster with an increased sliding speed from 1 to 3 cm/s, and then becomes faster with a further increased normal load to 5 N and slower with a further increased sliding speed to 5 cm/s under a lubrication condition. The friction and wear of the DLC-Steel tested at 3 cm/s under 1 N are lower than its friction and wear at 1 cm/s under 3 N, while its friction and wear tested at 5 cm/s under 3 N are also lower than its friction and wear at 3 cm/s under 5 N. It clearly indicates that the friction of the DLC-Steel is closely related to its wear under the dry condition, as its friction and wear tested against a 100Cr6 steel ball are more apparently influenced by the normal load under both dry and lubrication conditions.

The lowest friction of the DLC-Steel against a 100Cr6 steel ball with AFO is found at 3 cm/s under 5 N as a result of the most effective lubrication with the AFO, while its lowest dry friction exists at 1 cm/s under 1 N due to the combined effects of the lowest vibration of the tribo-test and the least wear damages of rubbing surfaces.

4. CONCLUSION

The friction and wear of the DLC-Steel produced via μW-PECVD were systematically investigated against a 100Cr6 steel ball without or with AFO at different sliding speeds of 1–5 cm/s under different normal loads of 1–5 N.

- At 3 cm/s under 3 N, the DLC-Steel against a 100Cr6 steel ball had a 57.8% lower friction coefficient under a dry condition and a 8.2% lower friction coefficient under a lubrication condition compared to those of the B-Steel against the same steel ball, indicating that the DLC coating apparently lowered the friction of the DLC-Steel than that of the B-Steel under both dry and lubrication conditions. The DLC-Steel itself had a 59.9% lower friction coefficient under the lubrication condition than under the dry condition due to the effective lubricating effect of the AFO.
- At 3 cm/s, increasing the normal load from 1 to 5 N resulted in a 18.7% increase in the friction coefficients of the DLC-Steel against a 100Cr6 steel ball under a dry condition as a result of the increased contact between two rubbing surfaces associated with their increased surface wear, but a 43.6% decrease in its friction coefficients under a lubrication condition via promoted lubrication with the AFO associated with its improved bearing surface.

- Under 3 N, the DLC-Steel tested dry had a 4.2% increase in its friction coefficient with an increased sliding speed from 1 to 3 cm/s as a result of its increased wear and then a 3.6% decrease in its friction coefficient with a further increased sliding speed to 5 cm/s via its decreased wear. However, the DLC-Steel had a 25.6% decrease in its friction coefficient with an increased sliding speed from 1 to 5 cm/s under a lubrication condition probably due to the promoted lubricating layer. The lowest friction of the DLC-Steel with the AFO was found at 3 cm/s under 5 N.

- At 3 cm/s under 3 N, the DLC-Steel had 85.1% lower wear than the B-Steel under a dry condition because of its higher wear resistant DLC coating than that of the steel. However, both B-Steel and DLC-Steel did not have any measurable wear under the lubrication condition.

- At 3 cm/s, increasing the normal load from 1 to 5 N resulted in a 417.9% increase in the wear of the DLC-Steel under a dry condition as a result of its increased wear.

- Under 3 N, increasing the sliding speed from 1 to 3 cm/s resulted in an 69.8% increase in the wear of the DLC-Steel without AFO due to the increased vibration of its tribo-system, but the further increased sliding speed to 5 cm/s resulted in a 13.3% decrease in its wear because the pronounced vibration of the tribo-system reduced its abrasive wear by lessening contact between two rubbing surfaces. Nevertheless, the DLC-Steel did not have any measurable wear for all the normal loads and sliding speeds under a lubrication condition.

- It could be concluded that the DLC-Steel could effectively prevent its underlying steel substrate from abrasive wear for all the normal loads and sliding speeds under both dry and lubrication conditions. The friction and wear of the DLC-Steel under both conditions were apparently influenced by the normal loads and sliding speeds, or, more precisely, by the normal loads.

REFERENCES

[1] M. Kalin, M. Polajnar, M. Kus, and F. Ma, "Green tribology for the sustainable engineering of the future," *Journal of Mechanical Engineering*, vol. 65, no. 11–12, pp. 709–727, Oct. 2019, doi: 10.5545/sv-jme.2019.6406.

[2] M. Freschi, A. Paniz, E. Cerqueni, G. Colella, and G. Dotelli, "The twelve principles of green tribology: studies, research, and case studies-a brief anthology," *Lubricants*, vol. 10, no. 6, pp. 129, June 2022, doi: 10.3390/lubricants10060129.

[3] K. Holmberg and A. Erdemir, "Influence of tribology on global energy consumption, costs and emissions," *Friction*, vol. 5, pp. 263–284, Sep. 2017, doi: 10.1007/s40544-017-0183-5.

[4] T. Haque, A. Morina, A. Neville, R. Kapadia, and S. Arrowsmith, "Non-ferrous coating/lubricant interactions in tribological contacts: Assessments of tribofilms," *Tribology International*, vol. 40, no. 10–12, pp. 1603–1612, Dec. 2007, doi: 10.1016/j.triboint.2007.01.023.

[5] F. Leach, G. Kalghatgi, R. Stone, and P. Miles, "The scope for improving the efficiency and environmental impact of internal combustion engines," *Transportation Engineering*, vol. 1, pp. 100005, Jun. 2020, doi: 10.1016/j.treng.2020.100005.

[6] H. Mahdisoozani, M. Mohsenizadeh, M. Bahiraei, A. Kasaeian, A. Daneshvar, M. Goodarzi, and M. R. Safaei, "Performance enhancement of internal combustion engines through vibration control: state of the art and challenges," *Applied Sciences*, vol. 9, no. 3, pp. 406, Jan. 2019, doi: 10.3390/app9030406.

[7] H. Jeon, "The impact of climate change on passenger vehicle fuel consumption: evidence from U.S. panel data," *Energies*, vol. 12, no. 23, pp. 4460, Nov. 2019, doi: 10.3390/en12234460.

[8] T. C. Austin, T. R. Carlson, and J. M. Lyones, "The benefits of reducing fuel consumption and greenhouse gas emissions from light duty vehicles," *SAE International Journal of Engines*, vol. 1, no. 1, pp. 480–490, 2009, doi: stable/26308297.

[9] M. Gallo and M. Marinelli, "Sustainable mobility: a review of possible actions and policies," *Sustainability*, vol. 12, no. 18, pp. 7499, Sep. 2020, doi: 10.3390/su12187499.

[10] L. Winkler, D. Pearce, J. Nelson, and O. Babacan, "The effect of sustainable mobility transition policies on cumulative urban transportation emissions and energy demand," *Nature Communications*, vol. 14, no. 2357, Apr. 2023, doi: s41467-023-37728-x.

[11] A. Neville, A. Morina, T. Haque, M. Voong, "Compatibility between tribological surfaces and lubricant additives: How friction and wear reduction can be controlled by surface/lube synergies," *Tribology International*, vol. 40, no. 10–12, pp. 1680–1695, Dec. 2007, doi: 10.1016/j.triboint.2007.01.019.

[12] V. W. Wong and S. C. Tung, "Overview of automotive engine friction and reduction trends: Effects of surface, material, and lubricant additive technologies," *Friction*, vol. 4, no. 1, pp. 1–28, Feb. 2016, doi: 10.1007/s40544-016-0107-9.

[13] F. Gustavsson, P. Forsberg, and S. Jacobson, "Friction and wear behavior of low friction coatings in conventional and alternative fuels," *Tribology International*, vol. 48, pp. 22–28, Apr. 2012, doi: 10.1016/j.triboint.2011.06.001.

[14] J. Vetter, "60 years of DLC coatings: Historical highlights and technical review of cathodic arc processes to synthesize various DLC types, and their evolution for industrial applications," *Surface and Coatings Technology*, vol. 257, pp. 213–240, Oct. 2014, doi: 10.1016/j.surfcoat.2014.08.017.

[15] J. Liu, Y. Zhang, B. Liao, "A review on preparation process and tribological performance of coatings for internal combustion engine piston rings," *Advances in Mechanical Engineering*, vol. 15, no. 5, pp. 1–19, May 2023, doi:10.1177/16878132231175752.

[16] M. S. Kabir, Z. Zhou, Z. Xie, and P. Munroe, "Scratch adhesion evaluation of diamond-like carbon coatings with alternate hard and soft multilayers," *Wear*, vol. 518–519, pp. 204647, Apr. 2023, doi: 10.1016/j.wear.2023.204647.

[17] D. K. Rajak, A. Kumar, A. Behera, and P. L. Menezes, "Diamond-like carbon coatings: Classification, properties, and applications," *Applied Sciences*, vol. 11, no. 4445, pp. 1–20, May 2021, doi: 10.3390/app11104445.

[18] S. V. Johnston and S. V. Hainsworth, "Effect of DLC coatings on wear in automotive applications," *Surface Engineering*, vol. 21, no. 1, pp. 67–71, Jul. 2013, doi: 10.1179/174329405X30039.

[19] A. Baptista, F. Silva, J. Porteiro, J. Miguez, and G. Pinto, "Sputtering physical vapour deposition coatings: A critical review on process improvement and market trend demands," *Coatings*, vol. 8, no. 11, pp. 402, Nov. 2018, doi: 10.3390/coatings8110402.

[20] K. L. Choy, "Chemical vapor deposition of coatings," *Progress in Materials Science*, vol. 48, no. 2, pp. 57–170, Jan. 2003, doi: 10.1016/S0079-6425(01)00009-3.

[21] L. Yin and Q. Chen, "The barrier properties of PET coated DLC film deposited by microwave surface-wave PECVD," *IOP Conference Series: Materials Science and Engineering*, vol. 274, no. 012042, 2017, doi. 10.1088/1757-899X/274/1/012042.

[22] J. Solis, H. Zhao, C. Wang, J. A. Verduzco, A. S. Bueno, and A. Neville, "Tribological performance of an H-DLC coating prepared by PECVD," *Applied Surface Science*, vol. 383, pp. 222–232, Oct. 2016, doi: 10.1016/j.apsusc.2016.04.184.

[23] N. W. Khun, A. Neville, and H. Zhao, "Effects of substrate bias on tribological properties of diamond-like carbon thin films deposited via microwave excited plasma enhanced chemical vapor deposition," *Journal of Tribology*, vol. 138, no. 3, pp. 031301, Jul. 2016, doi: 10.1115/1.4031995.

[24] M. Waqas, R. Zahid, M. U. Bhutta, Z. A. Khan, and A. Saeed, "A review of friction performance of lubricants with nano additives," *Materials*, vol. 14, no. 21, pp. 6310, Oct. 2021, doi. 10.3390/ma14216310.

[25] S. Kumar, C. M. S. Rauthan, P. N. Dixit, K. M. K. Srivatsa, M. Y. Khan, and R. Bhattacharyya, "Versatile microwave PECVD technique for deposition of DLC and other ordered carbon nanostructures," *Vacuum*, vol. 63, no. 3, pp. 433–439, Aug. 2001, doi: 10.1016/S0042-207X(01)00362-1.

[26] Y. Chen, P. Renner, and H. Liang, "A review of current understanding in tribochemical reactions involving lubricant additives," *Friction*, vol. 11, no. 4, pp. 489–512, Nov. 2022, doi: 10.1007/s40544-022-0637-2.

[27] W. Nishino, H. Uchida, and M. Yatsuzuka, "Reduction of pinhole defects in DLC film prepared with plasma based ion implantation and deposition," *Transitions of the Materials Research Society of Japan*, vol. 32, no. 4, pp. 887–890, Jan. 2007, doi: 10.14723/tmrsj.32.887.

[28] T. Maerten, C. Jaoul, R. Oltra, P. Duport, C. L. Niniven, P. Tristant, F. Meunier, and O. Jarry, "Micrometric growth defects of DLC thin films," *Journal of Carbon Research*, vol. 5, no. 4, pp. 73, Nov. 2019, doi: 10.3390/c5040073.

[29] A. LiBassi, A. C. Ferrai, V. Stolojan, B. K. Tanner, J. Roberson, and L. M. Brown, "Density, sp3 content, and internal layering of DLC films by X ray reflectivity and electron energy loss spectroscopy," *Diamond and Related Materials*, vol. 9, no. 3–6, pp. 771–776, May 2000, doi: 10.1016/S0925-9635(99)00233-2.

[30] J. Choi, S. Nakao, M. Ikeyama, J. Kim, and T. Kato, "Adhesion strength and optical transparency of DLC coatings on polycarbonate," *Transitions of the Materials Research Society of Japan*, vol. 32, no. 4, pp. 883–886, 2007.

[31] B. S. Giraldo, E. R. Parra, and P. J. A. Arango, "On the influence of a TiN interlayer on DLC coatings produced by pulsed vacuum arc discharge: Compositional and morphological study," *Applied Surface Science*, vol. 256, no. 1, pp. 136–141, Oct. 2009, doi: 10.1016/j.apsusc.2009.07.094.

[32] M. Zhang, X. G. Hu, X. X. Yang, F. F. Xu, K. H. Kim, and Z. G. Shao, "Influence of substrate bias on microstructure and morphology of ZrN thin films deposited by arc ion plating," *Transactions of Nonferrous Metals Society of China*, vol. 22, no. 1, pp. s115–s119, Oct. 2012, doi: 10.1016/S1003-6326(12)61694-X.

[33] B. V. Efremenko, V. I. Zurnadzhy, Y. G. Chabak, V. G. Efremenko, K. V. Kudinova, and V. A. Mazur, "A comparison study on the effect of counter ball material on sliding wear response of SLM printed biomedical 316L steel," *Materialstoday: Proceedings*, vol. 66, no. 4, pp. 2587–2593, Sep. 2022, doi: 10.1016/j.matpr.2022.07.112.

[34] N. W. Khun, W. Q. Toh, and E. Liu, "Study on changes in hardness and wear resistance of 3D printed Ti6Al4V with heat treatment temperature," *Tribology in Industry*, vol. 44, no. 1, pp. 129–135, Feb. 2023, doi: 10.24874/ti.1421.12.22.02.

[35] R. S. Godse, S. H. Gawande, and A. A. Keste, "Tribological behavior of high fraction carbon steel alloys," *Journal of Bio- and Tribo-Corrosion*, vol. 2, no. 3, Feb. 2016, doi: 10.1007/s40735-016-0034-3.

[36] H. H. Ding, V. Fridrici, J. Geringer, J. Fontaine, and P. Kapsa, "Low friction study between diamond like carbon coating and Ti6Al4V under fretting conditions," *Tribology International*, vol. 135, pp. 368–388, Jul. 2019, doi: 10.1016/j.triboint.2019.03.026.

[37] M. M. A. Asadi and H. A. A. Tameemi, "The effect of diamond-like carbon coating on the wear resistance at dry sliding conditions," *Materials Research Express*, vol. 9, no. 116504, Nov. 2022, doi: 10.1088/2053-1591/ac9bd4.

[38] F. F. Ling and R. C. Lucek, "On model studies of metallic surface asperities," *Journal of Applied Physics*, vol. 30, pp. 1559–1563, Oct. 1959, doi: 10.1063/1.1735000.

[39] I. Krupka and M. Hartl, "The effect of surface texturing on thin EHD lubrication films," *Tribology International*, vol. 40, no. 7, pp. 1100–1110, Jul. 2007, doi: 10.1016/j.triboint.2006.10.007.

[40] T. Zapletal, P. Sperka, I. Krupka, and M. Hartl, "The effect of surface roughness on friction and film thickness in transition from EHL to mixed lubrication," *Tribology International*, vol. 128, pp. 356–364, Dec. 2018, doi: 10.1016/j.triboint.2018.07.047.

[41] L. S. H. Chow and H. S. Cheng, "The effect of surface roughness on the average film thickness between lubricated rollers," *Journal of Tribology*, vol. 98, no. 1, pp. 117–124, Jan. 1976, doi: 10.1115/1.3452743.

[42] Z. Baccouch, R. Mnif, R. Elleuch, and C. Richard, "The effect of tribolayers on the behavior friction of X40CrMoV5/Fe360B steel couple in an open sliding contact," *Journal of Materials Research*, vol. 32, no. 13, pp. 2594–2600, Jul. 2017, doi: 10.1557/jmr.2017.81.

[43] R. Zhang, C. Zheng, C. Chen, B. Lv, G. Gao, Z. Yang, Y. Yang, and F. Zhang, "Study on fatigue wear competition mechanism and microstructure evolution on the surface of a bainitic steel rail," *Wear*, vol. 482–483, no. 203997, Oct. 2021, doi: 10.1016/j.wear.2021.203978.

[44] M. Vargova, M. Tavodova, K. Monkova, M. Dzupon, "Research of resistance of selected materials to abrasive wear to increase the ploughshare lifetime," *Metals*, vol. 12, no. 6, pp. 940, May 2022, doi: 10.3390/met12060940.

[45] M. M. D. O. Junior, H. L. Costa, W. M. S. Junior, and J. D. B. D. Mello, "Effect of iron oxide debris on the reciprocating sliding wear of tool steels," *Wear*, vol. 426–427, pp. 1065–1075, Apr. 2019, doi: 10.1016/j.wear.2018.12.047.

[46] T. Hisakado, "The influence of surface roughness on abrasive wear," Wear, vol. 41, no. 1, pp. 179–190, Jan. 1977, doi: 10.1016/0043-1648(77)90200-9.

[47] J. Robertson, "Diamond like amorphous carbon", *Materials Science and Engineering: R: Reports*, vol. 37, no. 4-6, pp. 129–281, May 2002, doi: 10.1016/S0927-796X(02)00005-0.

[48] Y. Liu, A. Erdemir, and E. I. Meletis, "An investigation of the relationship between graphitization and frictional behavior of DLC coatings," *Surface and Coatings Technology*, vol. 86-87, pp. 564–568, Dec. 1996, doi: 10.1016/S0257-8972(96)03057-5.

[49] I. Sugimoto, F. Honda, and K. Inouse, "Analysis of wear behavior and graphitization of hydrogenated DLC under boundary lubricant with MoDTC," *Wear*, vol. 305, no. 1–2, pp. 124–128, Jul. 2013, doi: 10.1016/j.wear.2013.04.030.

[50] Y. Liu, L. Wang, T. Liu, and P. Zhang, "Effect of normal loads and mating pairs on the tribological properties of diamond-like carbon film," *Wear*, vol. 486–487, no. 204083, Dec. 2021, doi: 10.1016/j.wear.2021.204083.

[51] C. Y. Nielsen, M. F. R. Zwicker, J. Spangenberg, N. Bay, and P. A. F. Martins, "The role of entrapped lubricant in asperity flattening under plastic deformation," *CIRP Annals*, vol. 71, no. 1, pp. 214–244, 2022, doi: 10.1016/j.cirp.2022.03.001.

[52] N. W. Khun, P. Q. Tan, A. W. Y. Tan, S. Wen, L. Erjia, and D. L. Buttler, "Effects of shot peen pressure on friction and wear of high pressure cold sprayed Ti6Al4V coatings under dry and lubrication conditions," *Tribology in Industry*, vol. 45, no. 3, pp. 472–486, Sep. 2023, doi: 10.24874/ti.1466.03.23.05.

[53] K. P. Lijesh and M. M. Khonsari, "On the degradation of tribo-components undergoing oscillating sliding contact," *Tribology International*, vol. 135, pp. 18–28, Jul. 2019, doi: 10.1016/j.triboint.2019.02.016.

[54] R. S. D. Joyce, B. W. Drinkwater, and C. J. Donohoe, "The measurement of lubricant-film thickness using ultrasound," *Proceedings: Mathematical, Physical, and Engineering Sciences*, vol. 459, no. 2032, pp. 957–976, Apr. 2003, doi: 3560015.

[55] L. Guo, P. L. Wong, and F. Guo, "Effects of viscosity and sliding speed on boundary slippage in thin film hydrodynamic lubrication," *Tribology International*, vol. 107, pp. 85–93, Mar. 2017, doi: 10.1016/j.triboint.2016.11.021.

[56] K. A. M. Aboua, N. Umehara, H. Kousaka, T. Tokoroyama, M. Murashima, M. M. B. Mustafa, Y. Mabuchi, T. Hiuchi, and M. Kawaguchi, "Effect of mating materials and graphitization on wear of a-C:H coating in boundary base oil lubrication," *Tribology Letters*, vol. 68, no. 24, Jan. 2020, doi: 10.1007/s11249-019-1248-6.

[57] H. Ronkainen, A. Laukkanen, and K. Holmberg, "Friction in a coated surface deformed by a sliding sphere," *Wear*, vol. 263, no. 7–12, pp. 1315–1323, Sep. 2007, doi: 10.1016/j.wear.2007.01.103.

[58] R. A. Poggie and J. J. Wert, "The influence of surface finish and strain hardening on near surface residual stress and the friction and wear behaviour of A2, D2 and CPM-10V tool steels," *Wear*, vol. 149, no. 1–2, pp. 209–220, Sep. 1991, doi: 10.1016/0043-1648(91)90374-4.